RESEARCH ARTICLE SUMMARY

SPECIATION

Rapid speciation via the evolution of pre-mating isolation in the Iberá Seedeater

Sheela P. Turbek*, Melanie Browne, Adrián S. Di Giacomo, Cecilia Kopuchian, Wesley M. Hochachka, Cecilia Estalles, Darío A. Lijtmaer, Pablo L. Tubaro, Luís Fábio Silveira, Irby J. Lovette, Rebecca J. Safran, Scott A. Taylor, Leonardo Campagna*

INTRODUCTION: Organisms in the early stages of speciation provide an opportunity to understand the processes that govern reproductive isolation between taxa. Ecological or behavioral mechanisms can serve as powerful barriers to the interbreeding of co-occurring species at the onset of their divergence. Tracking mating decisions within wild populations early in speciation can improve our understanding of how behavioral isolation promotes divergence.

RATIONALE: The southern capuchino seedeaters (*Sporophila*) are one of the most rapid avian radiations, showing remarkably low ecological and genomic divergence. We took advantage of the recent discovery of a capuchino species, the Iberá Seedeater (*S. iberaensis*), to study the origin and importance of pre-mating barriers early in speciation. By combining genomic and behavioral analyses, we examined (i) the role of assortative mating in the maintenance of species boundaries, (ii) the phenotypic traits underlying species recognition, (iii) the genomic basis of such traits, and (iv) the origin of these genomic variants.

RESULTS: *Sporophila iberaensis* was first observed in 2001 and co-occurs with *S. hypoxantha* throughout its main breeding location in the northern portion of the Iberá wetlands of Argentina. Across two breeding seasons, we located nests and collected genomic samples from both species. We found extremely low genome-wide differentiation, with the exception of three narrow regions located on different chromosomes. These regions contained 12 genes, three of which are involved in plumage coloration (*TYRP1*, *OCA2*, and *HERC2*). *Sporophila hypoxantha* and *S. iberaensis* males differ in coloration and song, but females are indistinguishable in coloration across the avian visual spectrum. We therefore used genomic data to quantify assortative mating. Each female's species-specific genotype always matched the genotype of her mate, demonstrating strong assortative mating despite these two species holding neighboring breeding territories, breeding synchronously, and foraging together on the same grasses. We tested the importance of divergent plumage patterning and song in species recognition and pre-mating isolation through playback experiments in the field. We presented territorial males with combinations of conspecific and heterospecific song and plumage, and assessed their aggressive behavioral responses. Each species responded most aggressively to conspecific song and plumage, confirming that both traits are used to recognize sexual competitors. Finally, we investigated the origin of the novel *S. iberaensis* plumage phenotype by examining genomic differentiation across the broader capuchino radiation. Although multiple species shared variants with *S. iberaensis* in the areas of elevated differentiation, the specific combination of these variants across the divergent regions distinguished *S. iberaensis* from all other capuchinos.

CONCLUSION: Our findings point to pre-mating isolation through assortative mate choice, based on both plumage coloration and song, as a primary mechanism promoting divergence between these co-occurring capuchino species. Although the ultimate fate of the incipient *S. iberaensis* species remains uncertain, our findings illustrate how lineages can form and quickly become reproductively isolated from co-occurring, syntopic species. Our results further suggest that the reshuffling of existing genetic variation can generate novel phenotypes that are then targeted by sexual selection. Assortative mating based on these traits may maintain species boundaries early in speciation while subsequent reproductive barriers accumulate. ■

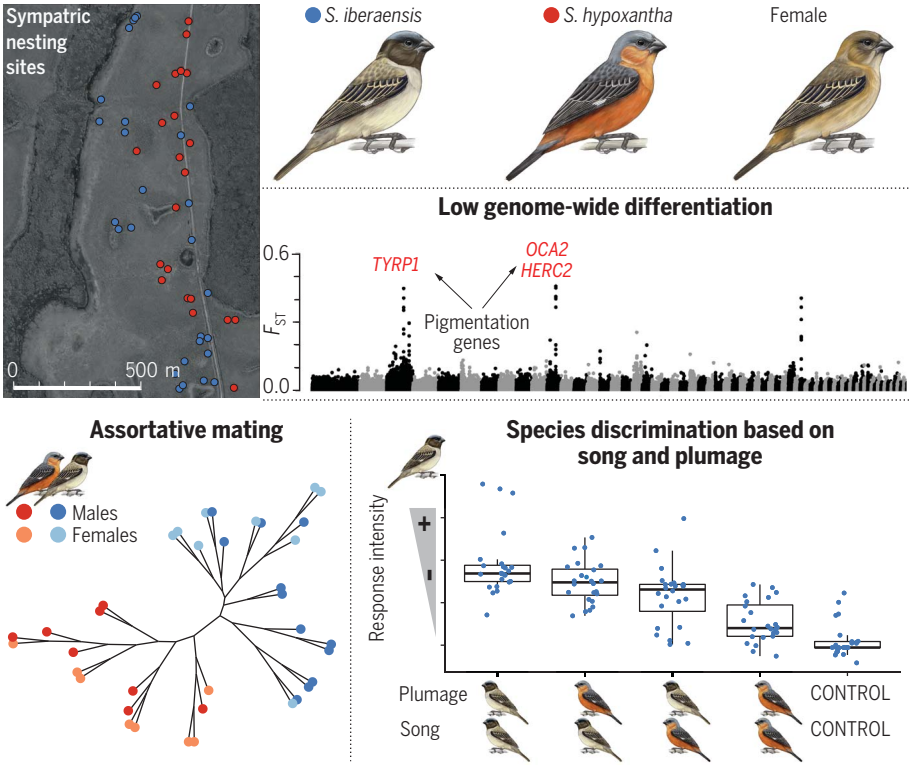

Novel mating signals restrict gene flow between co-occurring bird species. *Sporophila iberaensis* was first observed in 2001 and has a breeding range contained entirely within that of *S. hypoxantha*. Despite extremely low genomic differentiation, both species mate assortatively. Genetic differentiation is concentrated near genes known to be involved in plumage coloration. Field experiments show that both song and plumage are used to recognize sexual competitors.

The list of author affiliations is available in the full article online.
*Corresponding author. Email: sheela.turbek@colorado.edu (S.P.T.); lc736@cornell.edu (L.C.)
Cite this article as S. P. Turbek *et al.*, *Science* **371**, eabc0256 (2021). DOI: 10.1126/science.abc0256

READ THE FULL ARTICLE AT
https://doi.org/10.1126/science.abc0256

Downloaded from http://science.sciencemag.org/ on March 25, 2021

RESEARCH ARTICLE

SPECIATION

Rapid speciation via the evolution of pre-mating isolation in the Iberá Seedeater

Sheela P. Turbek[1]*, Melanie Browne[2], Adrián S. Di Giacomo[2], Cecilia Kopuchian[2], Wesley M. Hochachka[3], Cecilia Estalles[4], Darío A. Lijtmaer[4], Pablo L. Tubaro[4], Luís Fábio Silveira[5], Irby J. Lovette[6,7], Rebecca J. Safran[1], Scott A. Taylor[1], Leonardo Campagna[6,7]*

Behavioral isolation can catalyze speciation and permit the slow accumulation of additional reproductive barriers between co-occurring organisms. We illustrate how this process occurs by examining the genomic and behavioral bases of pre-mating isolation between two bird species (*Sporophila hypoxantha* and the recently discovered *S. iberaensis*) that belong to the southern capuchino seedeaters, a recent, rapid radiation characterized by variation in male plumage coloration and song. Although these two species co-occur without obvious ecological barriers to reproduction, we document behaviors indicating species recognition by song and plumage traits and strong assortative mating associated with genomic regions underlying male plumage patterning. Plumage differentiation likely originated through the reassembly of standing genetic variation, indicating how novel sexual signals may quickly arise and maintain species boundaries.

Organisms in the early stages of speciation provide an opportunity to understand the processes that govern reproductive isolation between taxa (*1*). Pre-mating isolation (e.g., ecological or behavioral mechanisms that prevent individuals from interbreeding) is a powerful barrier that can separate sympatric species early in divergence (*2*–*4*). Whereas post-mating barriers, such as genetic incompatibilities, take longer to accumulate than the time to speciation of many taxa (*5*, *6*), learned or genetic preferences can diverge over shorter time scales and generate assortative mating (*7*–*9*), fueling rapid speciation and paving the way for the accumulation of additional reproductive barriers (*3*, *6*, *10*). Tracking mating decisions among wild populations early in speciation can improve our understanding of how behavioral isolation promotes divergence.

Southern capuchino seedeaters (*Sporophila*) are one of the most rapid avian radiations, showing remarkably low levels of ecological and genomic divergence (*11*, *12*). Like Lake Victoria cichlids, where differences in male coloration promoted rapid diversification (*13*), the Neotropical southern capuchinos radiated within the past million years to form 10 predominantly sympatric species that differ primarily in male plumage coloration and song (*11*, *12*). Field experiments suggest that divergent male traits govern conspecific recognition and territorial defense (*14*). Nonetheless, viable hybrids between capuchino species are readily produced in the field (*15*) and in captivity (*16*), suggesting a lack of genetic incompatibilities.

Here, we take advantage of the identification of *S. iberaensis* (the Iberá Seedeater), a newly described species from Iberá National Park, Argentina, where six other southern capuchinos co-occur during the breeding season (*17*), to study the importance of pre-mating barriers early in speciation. *Sporophila iberaensis* was first observed in October 2001 (*18*), has a breeding range contained entirely within that of *S. hypoxantha* (Fig. 1, A and B, and fig. S1), and breeds primarily in the northern portion of the Iberá wetlands (in the 111,000-ha San Nicolás Reserve), where both species hold neighboring territories. Unlike its congeners, *S. iberaensis* is increasing in local abundance (Fig. 1C and fig. S1C). The species' breeding range is small, and until two decades ago this region was unexplored from an ornithological perspective because of a lack of public roads; these facts suggest that *S. iberaensis* likely already existed in the area and went undescribed (see supplementary text). This is consistent with other southern capuchino species that have small and restricted breeding ranges [e.g., *S. melanogaster* and *S. nigrorufa* (fig. S1A) (*17*)] and another more distantly related species in this taxonomically challenging genus (*S. beltoni*), which has a limited breeding range and was only recently identified in South America (*19*).

Throughout two breeding seasons, we located and monitored 128 nests of *S. hypoxantha* and *S. iberaensis*, the only two southern capuchinos observed successfully breeding in the San Nicolás Reserve in Iberá National Park during the study (Fig. 1, D and E, and table S1). We collected samples for genomic analyses from 80 nestlings and 126 adults and performed behavioral experiments with these two species to examine (i) the role of assortative mating in the maintenance of species boundaries, (ii) the phenotypic traits underlying species recognition, (iii) the genomic basis of such traits, and (iv) the origin of these genomic variants.

S. hypoxantha and *S. iberaensis* show low genomic differentiation

We examined the degree of genomic divergence between these species using shotgun short-read whole-genome sequences from 16 individuals of *S. hypoxantha* and 21 individuals of *S. iberaensis* (20 males and 17 females; table S2), identifying ~13.3 million single-nucleotide polymorphisms (SNPs). The 42 SNPs showing the highest differentiation [fixation index (F_{ST}) > 0.85, max = 0.94] were concentrated in three relatively narrow (30 to 50 kb) divergence peaks, which were located on separate chromosomes (1, 11, and sex chromosome Z; Fig. 1F) and exhibited increased absolute sequence divergence (D_{XY}; fig. S2). As among other capuchinos (*11*), *S. hypoxantha* and *S. iberaensis* are characterized by extremely low genomic differentiation (mean F_{ST} = 0.006 ± 0.059 SD) and no mitochondrial divergence (fig. S3). However, individuals clustered by species in a genome-wide principal components analysis (PCA; fig. S4). Individuals also clustered by species in separate PCAs performed with the SNPs from each peak (Fig. 1, G to I), but only one peak completely differentiated the two species (scaffold 430; Fig. 1H). Despite being located on different chromosomes, the three regions showed high values of linkage disequilibrium within and among the peaks (fig. S5), indicating their co-inheritance.

The lack of fixed differences (i.e., F_{ST} = 1) between *S. iberaensis* and *S. hypoxantha* among the 42 highly differentiated SNPs identified in our genome-wide F_{ST} analysis motivated us to search for the extent of shared variants between the species in the divergence peaks. We used polymerase chain reaction amplification to enable Sanger sequencing of a ~700–base pair (bp) region that included 15 of the 64 SNPs with F_{ST} greater than 0.79 within the peak on scaffold 430 (mean F_{ST} = 0.872 ± 0.028 SD); this allowed us to assess the genetic variation in this region for a sample of 202 individuals. We observed 21 of 200 *S. iberaensis* haplotypes that grouped with those of *S. hypoxantha* (Fig. 2). Although each species had a common haplotype, a few *S. iberaensis* individuals carried the *S. hypoxantha* haplotype, and a small proportion of haplotypes appeared to be intermediate. Some of the intermediate haplotypes belonged to *S. iberaensis* individuals and clustered with *S. hypoxantha*, yet

[1]Department of Ecology and Evolutionary Biology, University of Colorado, Boulder, CO, USA. [2]Centro de Ecología Aplicada del Litoral (CECOAL, CONICET), Corrientes, Argentina. [3]Center for Avian Population Studies, Cornell Lab of Ornithology, Ithaca, NY, USA. [4]Museo Argentino de Ciencias Naturales Bernardino Rivadavia (MACN, CONICET), Buenos Aires, Argentina. [5]Museu de Zoologia da Universidade de São Paulo, São Paulo, Brazil. [6]Department of Ecology and Evolutionary Biology, Cornell University, Ithaca, NY, USA. [7]Fuller Evolutionary Biology Program, Cornell Lab of Ornithology, Ithaca, NY, USA.
*Corresponding author. Email: sheela.turbek@colorado.edu (S.P.T.); lc736@cornell.edu (L.C.)

Downloaded from http://science.sciencemag.org/ on March 25, 2021

we also observed intermediate haplotypes in *S. hypoxantha* that did not cluster with *S. iberaensis* (Fig. 2). We obtained similar results when conducting this haplotype-based analysis on the 37 individuals with whole-genome sequencing data for all the variants found in the peak on scaffold 430 (fig. S6) and the SNPs showing the highest level of differentiation within the peaks on scaffolds 430 (fig. S7) and 257 (fig. S8 and supplementary text). Taken together, these findings are consistent with *S. hypoxantha* variants segregating within *S. iberaensis* at the sites showing the highest differentiation between the two species (and to a lesser extent in the reverse direction), which we attribute to either incomplete lineage sorting or past events of hybridization.

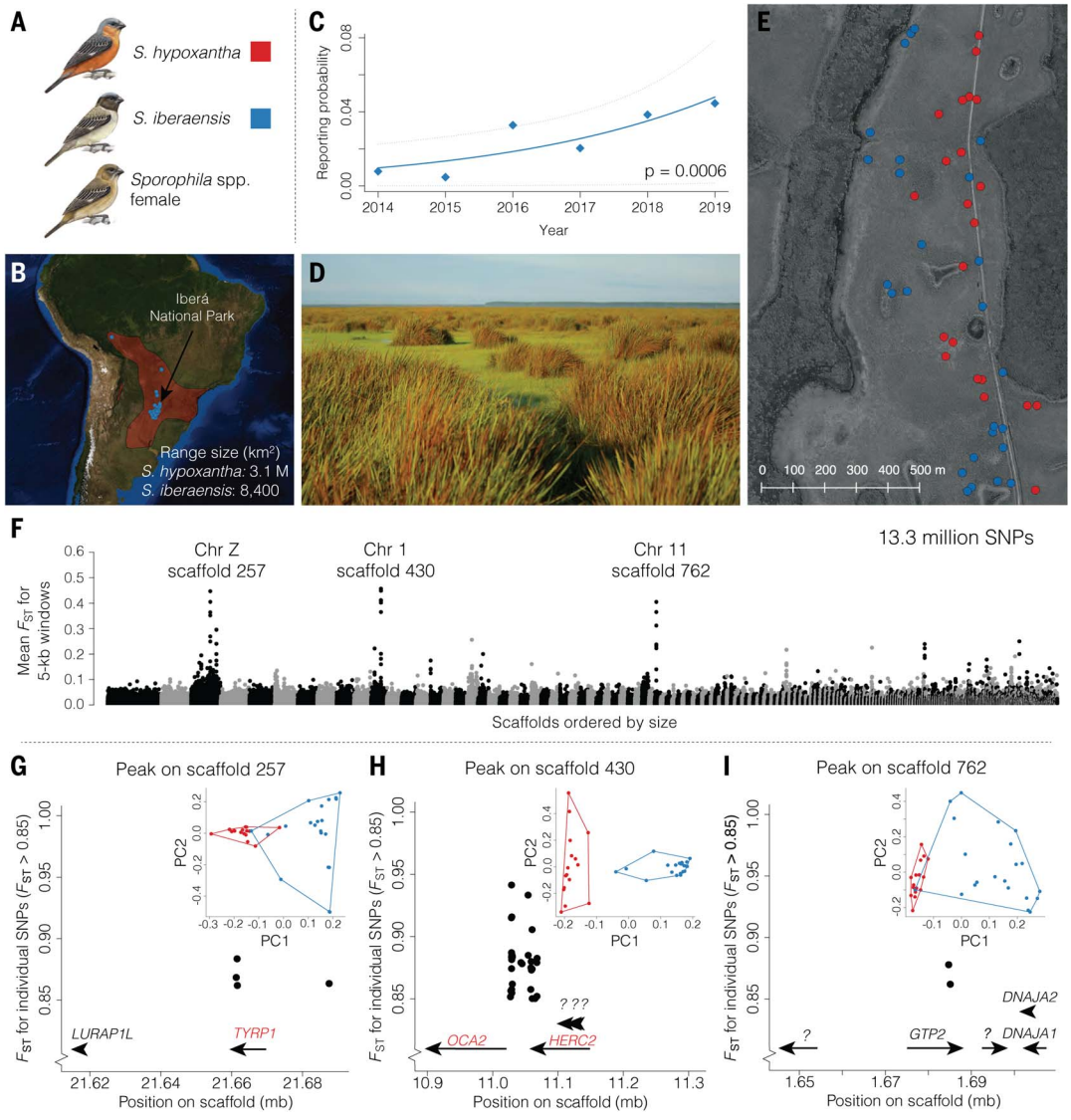

Fig. 1. Geographic context and genomic characterization of the study species. (**A**) Plumage phenotypes. (**B**) Breeding distribution of *S. hypoxantha* (red) (*17*) and *S. iberaensis* (blue circles are observations in the eBird database). The arrow indicates the study site location. (**C**) Increase in reporting rate probability for *S. iberaensis* in the eBird database (dotted lines are 95% prediction intervals for the estimated probabilities). (**D**) Typical breeding habitat. (**E**) Spatial distribution of 49 of the 128 nests of *S. hypoxantha* and *S. iberaensis* found during the study. (**F**) Pattern of genomic differentiation between individuals of *S. hypoxantha* (N = 16) and *S. iberaensis* (N = 21). Divergence peaks are labeled according to their scaffold and corresponding chromosome in the zebra finch assembly. The plot contains the 733 largest scaffolds. (**G** to **I**) Genomic locations of individual SNPs with F_{ST} > 0.85 on scaffolds 257, 430, and 762, respectively. Genes within 50 kb of these SNPs are depicted with arrows drawn with their length proportional to the size of the gene, with genes involved in coloration highlighted in red. The insets show PCAs of the SNPs under the peaks.

Table 1. Regions of elevated genomic differentiation between the two species.

Scaffold	Chr.	Peak size (kb)	Highest F_{ST} (over 5-kb window)	Number of SNPs with F_{ST} > 0.85	Number of genes (known function)	Coloration genes	Coloration gene function
257	Z	50	0.533	4	2 (2)	*TYRP1*	Encodes an enzyme involved in the production of melanin (*89*–*92*)
430	1	45	0.485	36	5 (2)	*OCA2*, *HERC2*	*OCA2* encodes a melanosomal transmembrane protein (*93*–*95*); *HERC2* contains a regulatory sequence that controls *OCA2* expression (*96*)
762	11	30	0.435	2	5 (3)	—	—

Downloaded from http://science.sciencemag.org/ on March 25, 2021

Divergence peaks contain plumage coloration genes

We identified 12 genes within the divergence peaks (Fig. 1, G to I, and Table 1). Two peaks (scaffolds 257 and 430) contained genes known to be involved in melanic coloration (*TYRP1*, *OCA2*, and *HERC2*; Fig. 1, G to I, and Table 1) (*20*). Most highly differentiated SNPs (98%) were located in noncoding regions (table S3), which may contain cis-regulatory elements that generate phenotypic variation (*11*). Although genes of small effect located outside of the divergence peaks could contribute to phenotypic differentiation, only 1.4% of SNPs in the genome had moderate F_{ST} values (F_{ST} > 0.2; fig. S9), which suggests that high differentiation is largely confined to the F_{ST} peaks.

S. hypoxantha and *S. iberaensis* mate assortatively in sympatry

S. hypoxantha and *S. iberaensis* females do not show clear morphological characters that allow their identification to one species or the other. However, given that birds can detect wavelengths in the ultraviolet range (300 to 400 nm) that are not perceived by humans (*21*), we examined the extent to which females of *S. hypoxantha* and *S. iberaensis* overlap in plumage coloration from an avian visual perspective. Benites *et al.* (*22*) detected coloration differences among females of four capuchino species that could be perceived by birds; however, we found that a large percentage of the convex hulls encompassing females of *S. iberaensis* in tetrahedral color space (a model of avian vision) were contained within those of *S. hypoxantha*, and the species largely overlapped in coloration across the avian visual spectrum (Fig. 3). Therefore, we used the divergent genomic regions to identify females to species and quantify assortative mating. Paired males and females (N = 17 pairs) clustered together in a tree derived from whole-genome data (Fig. 4A) and shared the same F_{ST} peaks (fig. S10), indicating a lack of hybrid pairs. We expanded this analysis to pairs for which we lacked whole-genome data (N = 23) by using double-digest restriction site–associated DNA (ddRAD) sequencing to genotype all sampled males, females, and nestlings (N = 206) at ~61,500 SNPs. Despite the extremely shallow genomic differentiation between these species, individuals clustered into two groups in a PCA, matching the phenotype of the male attending each nest (Fig. 4B). This signal was derived mainly from the cumulative effect of SNPs with low F_{ST} values, as the ddRAD data only contained 28 SNPs that fell within the F_{ST} peaks identified from the whole-genome data (fig. S11A) and showed the same pattern when those SNPs were excluded from the PCA (fig. S11B).

Because mating outside of the social pair bond is common in birds (*23*), we also used 281 highly informative ddRAD loci to evaluate patterns of paternity. Although the rate of extra-pair mating was very high (>52%; 35/67 offspring with known social fathers), all extra-pair offspring that matched candidate fathers in the dataset were sired by males of the same species as their social father (N = 18; table S4). In addition, both social (N = 40) and genetic pairs (N = 27) clustered by species according to their genomic PC1 score (Fig. 4C), indicating that assortative mating is maintained via both social and extra-pair mating.

Species discrimination is based on plumage and song traits

Sporophila hypoxantha and *S. iberaensis* mate assortatively despite holding neighboring territories during the breeding season (Fig. 1E), breeding synchronously (fig. S12), and foraging together on the same grasses (*24*). In addition to male plumage patterning, capuchinos differ in song (fig. S13), a culturally transmitted trait acquired primarily through social learning in songbirds, although there is a genetic component of early song discrimination (*25*). Therefore, differences in male plumage patterning and song, rather than temporal or spatial barriers to reproduction, likely mediate mate choice and prevent interbreeding through genetic and/or imprinting mechanisms (*4*, *9*, *14*).

To test the roles of divergent plumage patterning and song in species recognition and pre-mating isolation, we presented territorial males of *S. hypoxantha* (N = 40) and *S. iberaensis* (N = 36) with all combinations of conspecific and heterospecific capuchino song and plumage (using song playback and artificial mounts; see Fig. 5, A to C, and fig. S14), as well as song playback and artificial mounts of a sympatric and ecologically similar heterospecific control (*S. collaris*), and

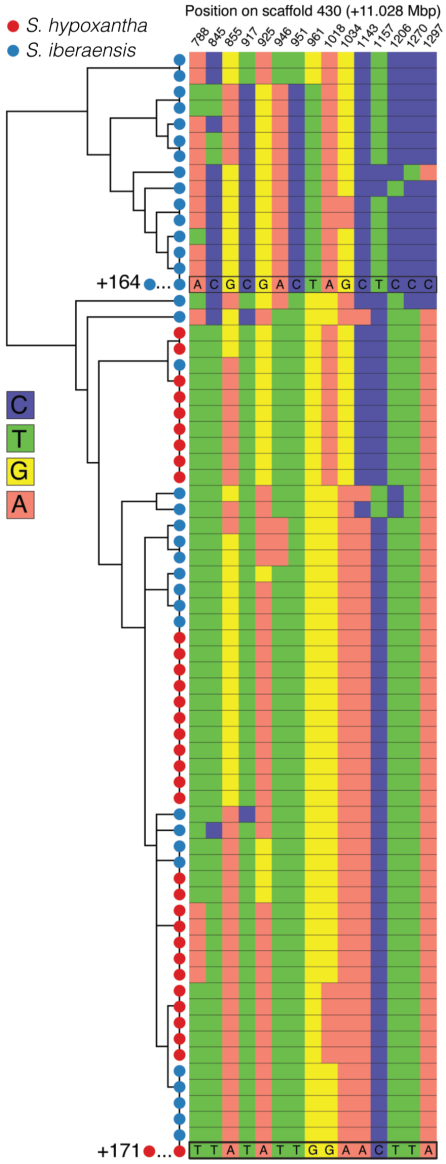

Fig. 2. Clustering of haplotypes obtained from the region of highest differentiation on scaffold 430. Phased genotypes of males, females, and nestlings of *S. hypoxantha* and *S. iberaensis* (N = 202) for 15 highly divergent SNPs located in the peak on scaffold 430 were generated from either whole-genome or Sanger sequence data (~700 bp). Each row represents a single chromosome, and each individual is represented twice in the tree. The four nucleotides are color-coded as indicated at left. *S. hypoxantha* individuals and the majority of *S. iberaensis* birds have species-specific haplotypes. However, 17/100 (17%) *S. iberaensis* birds possessed one haplotype that clustered with *S. hypoxantha*, and two *S. iberaensis* individuals (2%) clustered with *S. hypoxantha* on the basis of both haplotypes. The most common haplotype for each species is indicated at the bottom of the two main clusters. For graphical clarity, identical copies of each of these common haplotypes were omitted from the tree.

Downloaded from http://science.sciencemag.org/ on March 25, 2021

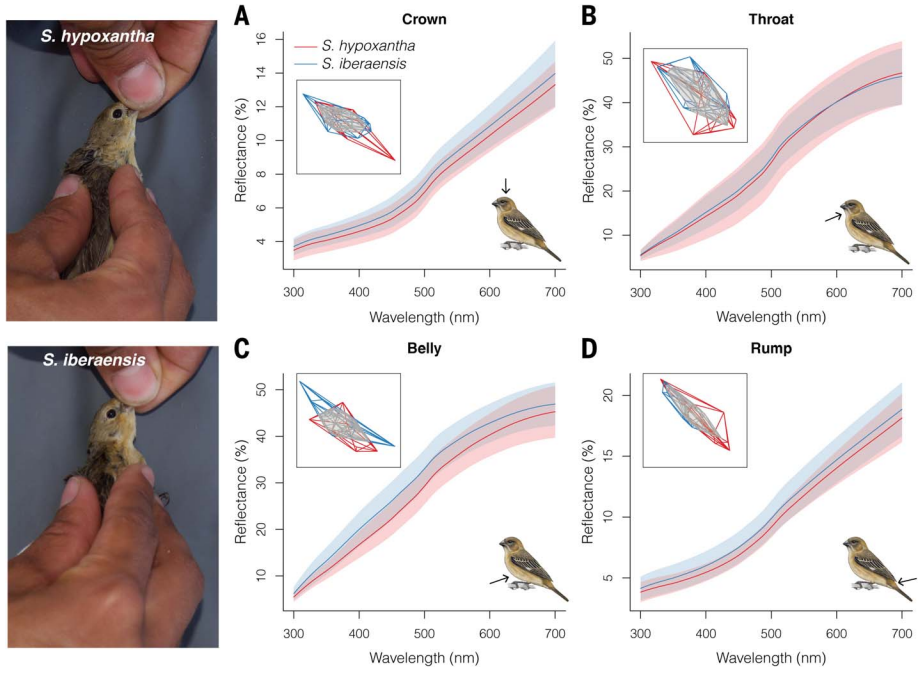

Fig. 3. Females of *S. hypoxantha* and *S. iberaensis* overlap in plumage coloration. (**A** to **D**) Phenotype, degree of overlap, and reflectance patterns across the avian visual spectrum for the crown (A), throat (B), belly (C), and rump (D) of *S. hypoxantha* (*N* = 22) and *S. iberaensis* (*N* = 20) females. Lines and shaded areas indicate mean reflectance ± SD for each group. The gray polygons in the insets show the extent of overlap in tetrahedral color space between the two species for the crown (43%), throat (72%), belly (58%), and rump (83%).

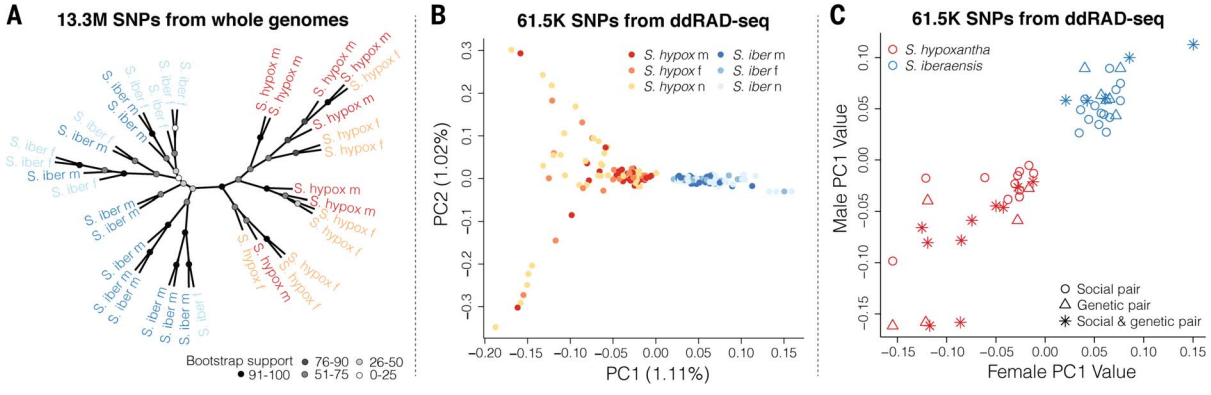

Fig. 4. No evidence of hybridization through social or extra-pair mating. (**A**) Whole-genome coalescent tree showing the relationship between males and females of *S. hypoxantha* and *S. iberaensis* (*N* = 37). (**B**) PCA from ddRAD sequencing data depicting genomic differentiation in males, females, and nestlings of *S. hypoxantha* and *S. iberaensis* (*N* = 206). (**C**) Genomic PC1 scores of males and females of *S. hypoxantha* and *S. iberaensis* for social (*N* = 40) and genetic pairs (*N* = 27; i.e., pairs that fertilized within-pair or extra-pair offspring). For all plots, females were classified according to the phenotype of their social mate.

assessed their behavioral responses. Across 240 trials (24 per treatment for each species), we recorded aggressive behaviors and generated a response intensity score using PCA (fig. S15). Each species responded most aggressively to the combination of conspecific song and plumage, exhibited intermediate responses to the treatments with mismatched traits, and largely ignored the heterospecific capuchino traits and those of the control species (Fig. 5, D and E, fig. S16, and table S5). Generalized linear mixed models confirmed that both song and plumage are used to recognize sexual competitors, with significant effects on the intensity of the males' response (song, $P < 0.0001$; plumage, $P < 0.0001$) and attack behavior (song, $P = 0.005$; plumage, $P = 0.012$) in both species (Table 2).

Existing mutations in novel combinations underlie the plumage phenotype of *S. iberaensis*

To investigate the origin of the novel *S. iberaensis* plumage phenotype, we examined genomic differentiation across the broader capuchino radiation (~28.2 million SNPs across 127 individuals from 12 species). We generated phylogenies using maximum likelihood for the entire genome and the regions containing divergence peaks. The whole-genome tree showed patterns consistent with recent speciation (Fig. 6A and fig. S17), such as a lack of species-level monophyly possibly due to hybridization and incomplete lineage sorting; this result was further supported by demographic modeling (fig. S18 and supplementary text). Despite this phylogenetic uncertainty, *S. iberaensis* formed a clade, as did most individuals from other species with restricted ranges [see *S. melanogaster* (green) and *S. nigrorufa* (yellow), Fig. 6A and fig. S17]. In contrast, *S. iberaensis* did not form a species-specific clade in the phylogenies derived from the regions containing divergence peaks (arrows in Fig. 6, B and C, and fig. S19), unlike most individuals of *S. melanogaster* (indicated with a circle in Fig. 6B) and *S. ruficollis* (indicated with a circle in Fig. 6C). Although multiple species shared variants with *S. iberaensis* at the individual divergence peaks (e.g., *S. ruficollis* in peak 257 and five other species in peak 430; Fig. 6, B and C, and fig. S19), the particular combination found only in *S. iberaensis* distinguished it from other capuchinos (note that no other capuchino shares variants with *S. iberaensis* at both divergence peaks; Fig. 6, B

Downloaded from http://science.sciencemag.org/ on March 25, 2021

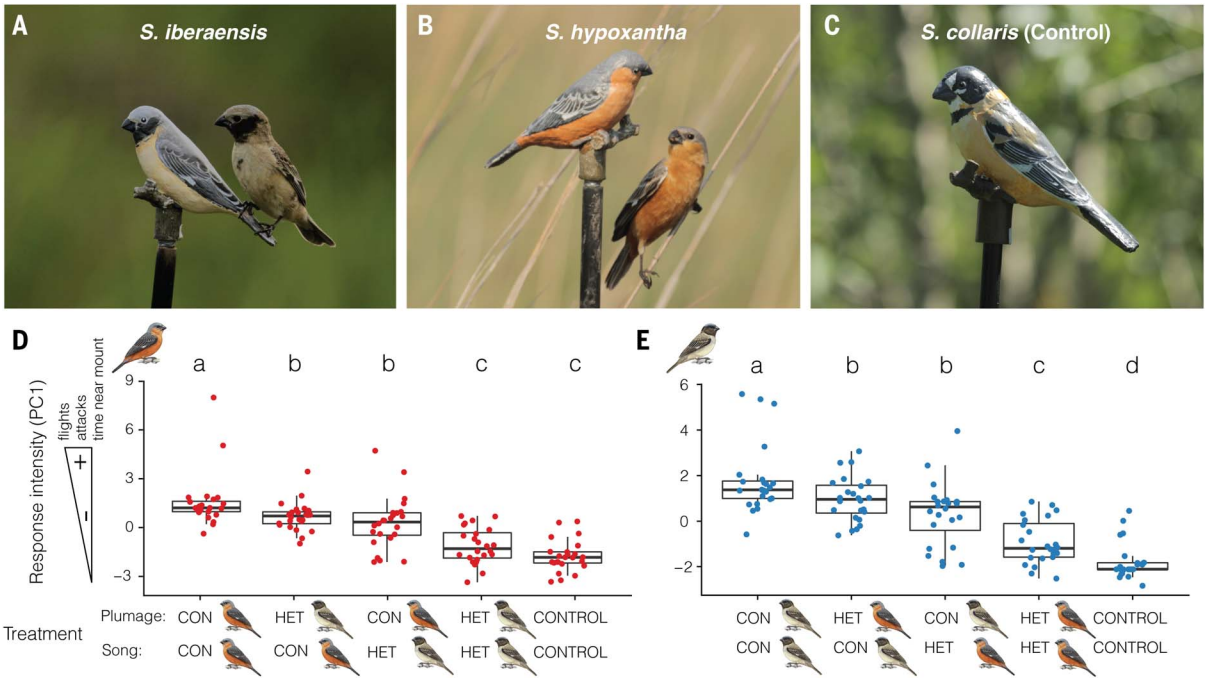

Fig. 5. Territorial males of both species respond most aggressively to conspecific song and plumage. (**A** to **C**) Artificial mounts of *S. iberaensis* (A), *S. hypoxantha* (B), and *S. collaris* (the control) (C) alongside breeding males of the two capuchino species. Two mounts were created per species for use in the behavioral experiment. (**D** and **E**) Behavioral response intensity (PC1) of territorial males of *S. hypoxantha* and *S. iberaensis*, respectively, to combinations of conspecific (CON), heterospecific capuchino (HET), and control (CONTROL) song and plumage. Different letters indicate statistical significance between treatment groups (adjusted $P < 0.05$, $N = 120$ per species; Tukey's HSD test).

and C, and fig. S20). This result implies that the *S. iberaensis* phenotype likely arose through the reshuffling of standing genetic variation that already existed within the other southern capuchinos, providing a mechanism for rapid speciation without the long period required for relevant mutations to arise de novo (*26*, *27*).

Discussion

Our findings point to pre-mating isolation through assortative mate choice, based on genetically inherited (plumage color) and culturally inherited traits [song, but see (*25*)], as a primary mechanism promoting divergence between these co-occurring capuchino species. Although we never observed hybrid pairs during this study, selection against intermediate traits (plumage patterns or songs) or mismatched plumage and song traits in hybrids could further strengthen assortative mating through reinforcement (*28*). Most divergence peaks in capuchinos (*11*) and one of the three peaks between *S. iberaensis* and *S. hypoxantha* are located on the sex chromosome Z. Loci on sex chromosomes are thought to have a disproportionate effect on hybrid fitness [large-Z effect (*29*)] and may have played a predominant role in the evolution of the southern capuchino radiation. Functional studies of specific variants in these divergent genomic regions will help to clarify how novel allele associations could lead to different plumage phenotypes. Although the ultimate fate of the incipient *S. iberaensis* species remains uncertain, our findings illustrate how phenotypically differentiated lineages can form and rapidly become reproductively isolated from co-occurring, syntopic species (*30*, *31*). Our results suggest that the reshuffling of standing genetic variation can generate novel phenotypes that are targeted by sexual selection. Assortative mating based on these traits may maintain species boundaries early in speciation while subsequent reproductive barriers accumulate.

Materials and methods

Field methods

We have carried out extensive field work in Iberá National Park (Argentina) since 2007, encountering individuals of all seven southern capuchino seedeaters that breed in the region. In the San Nicolás Reserve (28°07′ 41.4″ S, 57°26′04.7″ W), where this study took place, our group has conducted studies on the breeding ecology of capuchinos since 2014. During the study, *S. hypoxantha* and *S. iberaensis* were the only two southern capuchino species observed successfully breeding in San Nicolás. From November 2016 to January 2017 and from October to December 2018, we located and monitored 128 nests of the two species (*S. hypoxantha*, $N = 65$; *S. iberaensis*, $N = 63$). We collected blood samples from the brachial veins of 126 adults and 77 nestlings (*S. hypoxantha*, $N = 40$ adult males, 23 adult females, 40 nestlings; *S. iberaensis*, 42 adult males, 21 adult females, 37 nestlings), as well as tissue samples from two unhatched eggs of *S. hypoxantha* and one unhatched egg of *S. iberaensis* (table S1). In addition, we collected feather samples from four plumage patches across the body (crown, throat, belly, and rump) of individuals of *S. hypoxantha* ($N = 46$ males, 22 females) and *S. iberaensis* ($N = 41$ males, 20 females) to examine plumage coloration (described below). Males were attracted with playback and captured with mist nets during the nest construction, egg laying, and nestling provisioning stages; females were captured at the nest during nestling provisioning. We measured and banded each individual with a numbered aluminum band and specific combination of colored leg bands prior to release. Blood samples were stored in lysis buffer and DNA was extracted with DNeasy blood and tissue kits (Qiagen) for all subsequent genomic analyses. From October to December 2019, we carried out an additional behavioral experiment in the San Nicolás Reserve (described below) to test the importance of song and plumage coloration in species recognition and pre-mating isolation between *S. hypoxantha* and *S. iberaensis*.

Capuchino seedeaters are austral migrants that breed in the Iberá wetlands and migrate

Downloaded from http://science.sciencemag.org/ on March 25, 2021

Table 2. Species discrimination is based on both plumage and song. Data are generalized linear mixed model results examining the behavioral responses of territorial males of *S. hypoxantha* and *S. iberaensis* to mount presentations and song playbacks when the heterospecific control (*S. collaris*) trials were excluded. Significant results ($P < 0.05$) are in boldface. Plumage (conspecific versus heterospecific) and Song (conspecific versus heterospecific) had a significant effect on response intensity, regardless of whether outliers (observations outside 1.5 × interquartile range) in each treatment group were included ($N = 192$) or excluded ($N = 179$; Plumage, $P < 0.0001$; Song, $P < 0.0001$), whereas the species of the focal male did not affect behavioral response. We detected an additional significant interaction between Song and Plumage on response intensity ($P = 0.03$) when outliers were removed, which could indicate a synergistic effect when both traits belong to the same species. For response intensity, the model included male ID (SD = 0.89; 95% CI of SD = 0.70 to 1.12) and female presence (SD = 0.26; 95% CI of SD = 0.03 to 1.21) as random effects. For attack behavior, the model included male ID (SD = 2.90; 95% CI of SD = 1.34 to 6.28) as a random effect.

Response intensity (PC1)	**Estimate**	**SE**	***t* value**	***P* value**
Intercept	−1.63	0.29	−5.70	**0.0007**
Species	−0.16	0.26	−0.62	0.535
Plumage	0.93	0.18	5.04	**<0.0001**
Song	1.41	0.19	7.58	**<0.0001**
Plumage × Song	0.24	0.26	0.92	0.360
Attack behavior	**Estimate**	**SE**	***z* value**	***P* value**
Intercept	0.11	0.78	0.14	0.889
Species	1.19	1.00	1.20	0.232
Plumage	−2.76	1.10	−2.52	**0.012**
Song	−3.19	1.14	−2.79	**0.005**
Plumage × Song	−20.38	12,802.17	−0.002	0.999

northward during the nonbreeding season (*32*). Over the course of the breeding season in 2018, we resighted nine individuals (16%) of *S. hypoxantha* ($N = 4$) and *S. iberaensis* ($N = 5$) of the 56 adults that were banded in 2016, two breeding seasons prior. In addition, in 2019, we resighted 22 banded males (26%) of *S. hypoxantha* ($N = 12$) and *S. iberaensis* ($N = 10$) of the 86 males banded during 2016–2018. Almost all of the resighted males were holding territories in the same geographic area of the study site as in previous breeding seasons. This relatively low recapture rate, but high philopatry, may be attributed to low interannual survival and demonstrates high turnover in the individuals that are present at the breeding site across different years. The combination of a low recapture rate and the fact that females are indistinguishable to the human eye makes it difficult to quantify assortative mating by directly tracking the mating decisions of banded individuals across years (see below).

Whole-genome resequencing and variant discovery

We generated shotgun short-read whole-genome sequences for 37 individuals of *S. hypoxantha* ($N = 8$ males, 8 females) and *S. iberaensis* ($N = 12$ males, 9 females). Whole-genome resequencing generated more than 860 million paired-end reads with a length of 151 bp, producing an expected per-individual coverage ranging between 3.9× and 10.7× (median, 5.4×; table S2).

We evaluated the sequencing quality of individual libraries with FastQC (version 0.11.7) and used AdapterRemoval (version 2.1.7) to trim adapter sequences, filter by quality, and merge overlapping paired-end reads (*33*, *34*). The filtered data were aligned to a previously assembled reference genome of *S. hypoxantha* (*11*) using the "very-sensitive-local" option in Bowtie2 (version 2.3.4), and alignment statistics were subsequently obtained using Qualimap (version 2.2.1) (*35*, *36*). A high percentage of reads aligned to the reference genome (*S. hypoxantha*, mean = 98.6 ± 0.2% SD; *S. iberaensis*, mean = 98.6 ± 0.1% SD), and the average depth of coverage after filtering and alignment was 5.6× per sample (range, 3.8× to 10.3×; table S2).

We used SAMtools (version 1.7) to convert SAM to BAM files and sort and index the data (*37*). We then marked PCR duplicates with Picard Tools (version 2.17.10) and used HaplotypeCaller in GATK (version 3.8.0) to perform SNP variant discovery and genotyping (*38*, *39*). The following hard filtering parameters were used to exclude variants in GATK: QD < 2.0, FS > 60.0, MQ < 20.0, and ReadPosRankSum < −8.0. We additionally used VCFtools (version 0.1.13) to filter out variants that had a minor allele frequency of less than 8% (retaining alleles present in at least three homozygous individuals), a mean depth of coverage lower than 2 or greater than 50, more than 20% missing data, or were not biallelic (*40*). This pipeline produced 13,254,970 SNPs, and the average percent of missing data was 5% per individual.

Population genomics

To search for regions of elevated differentiation between *S. hypoxantha* and *S. iberaensis*, we computed average F_{ST} values for nonoverlapping 5-kb windows, as well as individual SNPs, using VCFtools. Peaks of divergence were identified as 5-kb windows with elevated genomic divergence that contained at least one individual SNP with $F_{ST} > 0.85$. This criterion focused on the strongest putative targets of divergent selection, although it may have excluded regions under selection that contained genes of small effect. We identified three peaks of divergence between the two species by building Manhattan plots and conducting PCAs of the genomic data with the packages *qqman* and *SNPRelate* in R version 3.5.2 (*41*–*43*). In addition, we estimated D_{XY}, an absolute measure of divergence, over nonoverlapping 5-kb windows for the three peaks of divergence using the custom script popgenWindows.py (https://github.com/simonhmartin/genomics_general). We explored patterns of linkage disequilibrium in these regions by calculating the r^2 statistic in plink version 1.9 (*44*).

The reference genome was assembled to contigs from short-read shotgun and mate-pair libraries, and subsequently assembled to scaffolds using long-read data from Pacific Biosciences sequencing (*11*). Although some of these scaffolds are large, they are not assembled to chromosome level. To assign scaffolds with divergence peaks to chromosomes, we aligned them to the zebra finch assembly (Taeniopygia_guttata-3.2.4) using the Satsuma synteny model from Satsuma version 3.1 (*45*). We assigned each scaffold to the chromosome with the top hit and examined the results with MizBee (*46*). Finally, we referred to the annotated *S. hypoxantha* genome in (*11*) to compile a list of genes within 50 kb of each divergence peak and searched for these annotations of interest in the UniProt (www.uniprot.org/) and Human Gene databases (www.genecards.org) to identify genes in the regions of elevated differentiation. The gene *OCA2* is adjacent to *HERC2* in the zebra finch, yet was not annotated in the *S. hypoxantha* reference genome. We located the *OCA2* coordinates in our reference genome by aligning the zebra finch mRNA (XM_032749285.1) using BLAST (*47*). To search for areas that could play an important role in regulating the expression of *OCA2* (i.e., cis-regulatory elements), we assessed the level of conservation of the intergenic region between *OCA2* and *HERC2*, the area of the genome showing the highest differentiation between *S. iberaensis* and *S. hypoxantha*, with respect to more distantly related birds by using

Downloaded from http://science.sciencemag.org/ on March 25, 2021

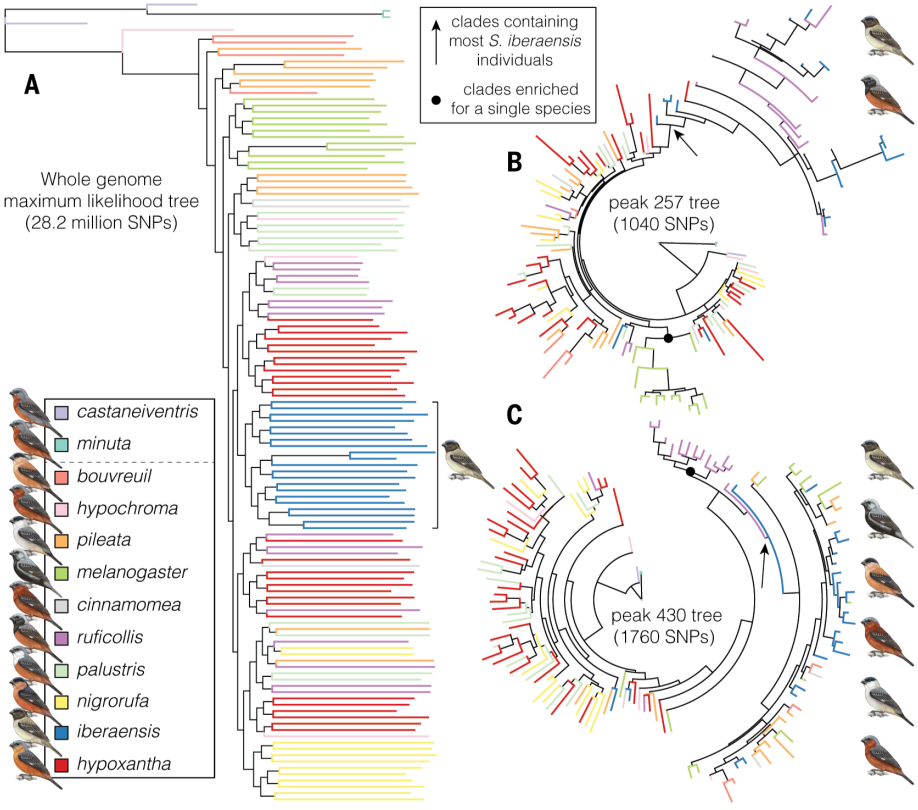

Fig. 6. *S. iberaensis* is monophyletic but shares variants at divergence peaks with other capuchinos. (**A** to **C**) Capuchino phylogeny inferred using maximum likelihood based on whole-genome data (A) and SNPs from the peaks on scaffold 257 (B) and scaffold 430 (C). The black square bracket and arrows indicate clades containing all or most *S. iberaensis* individuals; the black circles indicate clades of other species with species-specific variants at the peaks of differentiation. Outgroups are shown above the dashed line in the key at lower left.

the Bird PhastCons track (*48*) from the University of California, Santa Cruz, genome browser (*49*). Bird PhastCons scores are derived from a multigenome alignment of the budgerigar (*Melopsittacus undulatus*), zebra finch (*Taeniopygia guttata*), chicken (*Gallus gallus*), and turkey (*Meleagris gallopavo*) genomes, and represent the probability that a nucleotide belongs to a conserved element (ranging from 0 to 1). Areas that are highly conserved among distantly related species may contain regulatory elements that are important for controlling gene expression. We aligned the ~37 kb of sequence to the medium ground finch (*Geospiza fortis*) reference genome (geoFor1, to which the PhastCons scores were mapped) using BLAT (*50*) with a 96.4% identity.

In addition, we assembled full mitochondrial genomes from the filtered whole-genome sequences belonging to *S. hypoxantha* and *S. iberaensis* individuals with MITObim 1.9.1 (*51*), using the "quick" option and up to 40 iterations with the full mitochondrial genome from *Geospiza magnirostris* as a template (GenBank number NC_039770.1). We aligned the 37 individual sequences with an average length of 16,562 bp in Geneious version 10.1.3 (*52*) and subsequently constructed an unrooted statistical parsimony network using PopART 1.7 (*53*). In addition, we used the same methodology to generate a network from the recovered COI DNA barcodes, which are frequently used for species identification (*54*–*56*).

To generate phylogenetic hypotheses defined by the variants within the three divergence peaks in the context of the entire capuchino radiation, and to compare these relationships to those in a whole-genome phylogeny of all capuchino species, we increased our genomic sampling to the 10 southern capuchino species plus two outgroups. We combined the 37 whole-genome sequences obtained from *S. hypoxantha* and *S. iberaensis* with 72 additional individuals from nine capuchino species previously sequenced and published by Campagna *et al.* (*11*), 12 new individuals from *S. ruficollis* sequenced on a lane of Illumina NextSeq 500 (paired-end, 151 bp), and six additional individuals sequenced on a lane of Illumina NextSeq 500 (mid-output mode, paired-end, 151 bp). All additional sequencing was performed at the Cornell University Biotechnology Resource Center (BRC). We assembled a VCF file (as described above) with a total of 127 individuals (28 *S. hypoxantha*, 21 *S. iberaensis*, 15 *S. ruficollis*, 12 *S. pileata*, 12 *S. palustris*, 12 *S. melanogaster*, 12 *S. nigrorufa*, four *S. bouvreuil*, four *S. hypochroma*, three *S. cinnamomea*, and two individuals each of *S. minuta* and *S. castaneiventris* as outgroups). We applied the same hard filters as described above and subsequently retained variants that were present in 80% of all individuals, had a depth of coverage between 4 and 50, and had a minor allele count of at least four. This combined dataset contained 32,993,511 SNPs after filtering. We explored the relationships among individuals and species by performing a PCA in *SNPRelate* and used VCFtools to create three additional files with subsets of SNPs from the regions defined by each divergence peak (1760 SNPs for the peak on scaffold 430, 1040 SNPs for the peak on scaffold 257, and 13 SNPs for the peak on scaffold 762). We used RAxML version 8.2.4 (*57*) to produce maximum likelihood phylogenies from the variants of each of the three divergence peaks, implementing the "ASC_GTRGAMMA" model and the Lewis correction for ascertainment bias. For the more computationally demanding whole-genome phylogeny, we used RAxML-ng version 0.9.0 (*58*) and the "GTR+G+ASC_LEWIS" model. RAxML-ng used the 28.2 million SNPs that had the minor allele in homozygosity in at least one individual (from the total of ~33 million variants in the dataset). This analysis ran for ~1600 clock hours on all 64 cores of a computer with 512 Gb of RAM. Despite not converging on a single best phylogeny, an inspection of trees from the final search rounds showed very little variation, with only minor changes at the tips of the tree. We therefore generated a smaller dataset by applying more stringent filtering parameters (85% of individuals present at a locus and a minimum minor allele frequency of 10%), which retained 6,283,771 SNPs. We ran RAxML-ng on this

Downloaded from http://science.sciencemag.org/ on March 25, 2021

dataset under the same conditions as described above, except that we used a parsimony tree as a starting point. This strategy converged on a single best tree, and both datasets (28.2 million and 6.3 million SNPs) produced comparable topologies.

Double-digest restriction site-associated DNA sequencing

To determine species identity for individuals without whole-genome data, assign paternity, and analyze patterns of assortative mating, we sequenced 206 individuals (126 adults, 77 nestlings, and three unhatched eggs from 23 nests of *S. hypoxantha* and 20 nests of *S. iberaensis*) in two separate sequencing runs following the double-digest restriction site-associated DNA (ddRAD) sequencing protocol detailed in (*59*).

We used FASTX-Toolkit (http://hannonlab.cshl.edu/fastx_toolkit/) to trim the 3′ end of all reads to a length of 97 bp (FASTX Trimmer) and eliminated sequences (FASTX Quality Filter) if at least one base had a Phred score below 10 (90% call accuracy) or more than 5% of the bases had a score below 20 (99.9% call accuracy). We aligned the ddRAD data to the reference genome of *S. hypoxantha* using the 'sensitive' option in Bowtie2 (version 2.3.5) and sorted and indexed the data with SAMtools (version 1.9). We then used the *gstacks* and *populations* modules of Stacks (version 2.3) to call variants and remove loci that were present in fewer than 80% of individuals (*60*). The effective per-sample coverage was 31.8× ± 15.1× (mean ± SD). This pipeline produced a VCF file containing 61,484 SNPs across the 206 individuals.

Sanger sequencing of a region within the divergence peak on scaffold 430

To investigate the genomic architecture of phenotypic differences between the species in more detail, we developed a pair of primers (forward, 5′-ATTGCTGGTGTCTCCTTATTGA-3′; reverse, 5′-ATGTCCCTTTGGCTGTCTG-3′) to sequence a ~700-bp region on scaffold 430 (11,028,673 to 11,029,376 bp) that contained 12 highly divergent SNPs (F_{ST} > 0.85) and an additional three SNPs with F_{ST} > 0.79. We amplified the divergent region via PCR for 165 individuals (N = 87 adults, 77 nestlings, and one unhatched egg) with GoTaq colorless master mix (Promega) and the following thermal cycle profile: 3 min at 95°C, followed by 25 cycles of 30 s at 95°C, 30 s at 61°C, and 1 min at 72°C, and finally 5 min at 72°C. The PCR product was Sanger-sequenced in both directions with the same primers used for amplification at the Cornell University BRC.

We used Unipro UGENE version 1.32.0 to trim primers and edit the Sanger sequences (*61*) and combined the information from these sequences with variants obtained through whole-genome sequencing to determine the genotypes of 202 individuals at 15 SNPs that showed high levels of differentiation within the peak on scaffold 430. We calculated F_{ST} values at each site using VCFtools and subsequently phased and imputed missing data (~5.2% or 158 out of 3060 genotypes, with a mean probability of 0.996 ± 0036 SD) using BEAGLE version 3.3.2 (*62*). This resulted in 404 haplotypes, two per individual. We explored the relationships between individuals at these sites by calculating a distance matrix in the R package *vegan* (*63*) and plotting it with the function *phylo.heatmap()* from the R package *phytools* (*64*). We also compared these results to three similar plots derived from the *S. iberaensis* (N = 21) and *S. hypoxantha* (N = 16) individuals for which we had whole-genome sequencing data. We produced one plot for all SNPs found in the divergence peak on scaffold 430, one plot for the 64 SNPs with F_{ST} > 0.79 found in the same region, and a third plot for the 13 SNPs with F_{ST} > 0.79 found in the divergence peak on scaffold 257. We used an F_{ST} cutoff of 0.79, as the segment selected for PCR amplification included SNPs with this level of divergence.

Assortative mating

We analyzed patterns of social pairing from the whole-genome data (N = 17 social pairs) by first creating a tree of individuals using SVDquartets, implemented in PAUP*. SVDquartets is a coalescent-based method that compares possible quartet topologies for a set of four taxa, selecting the topology with the lowest score (*65*). In addition, we used the R package *qqman* to create Manhattan plots comparing the level of differentiation between species for males and females independently in each of the three divergence peaks. We evaluated whether individuals that formed a social pair grouped together on the tree, as expected if assortative mating contributes to reproductive isolation between *S. hypoxantha* and *S. iberaensis*, and showed elevated levels of differentiation in the same genomic regions.

For all social pairs (N = 40), including those with whole-genome data, we used the ddRAD pipeline to assign individuals to species and calculate the number of observed conspecific and heterospecific pairings. Specifically, we conducted a PCA of the genomic data using the *SNPRelate* package in R and evaluated whether (i) individuals clustered by species in a PCA, and (ii) socially or genetically determined male-female pairs (see below) grouped together by species on the basis of their diagnostic genomic PC1 scores.

Paternity analysis

We further filtered the VCF file from the ddRAD pipeline using the *populations* module of Stacks (version 2.3) to remove loci that had a minor allele frequency of less than 0.25 or an observed heterozygosity greater than 0.7, or were present in fewer than 95% of individuals. We restricted the analysis to the first SNP per locus and used VCFtools to remove loci that were not in Hardy-Weinberg equilibrium or had a mean depth of coverage below 20. This pipeline produced a VCF file containing 281 highly informative loci across the 206 individuals that we used for paternity analysis.

After filtering, we converted the VCF file to a format compatible with CERVUS 3.0.7, which takes a likelihood approach to assign paternity from SNP data (*66*). CERVUS calculates the natural logarithm of the likelihood ratio (LOD score) for each potential pairing by comparing offspring genotypes to the genotypes of candidate parents and random individuals in the population. The LOD score thus estimates the relative likelihood that a sampled offspring was sired by a candidate father rather than a random male in the population. In addition, the program conducts a simulated parentage analysis using population allele frequencies and the proportion of candidate parents sampled in the dataset to calculate the critical differences in LOD scores necessary to assign paternity with either 80% or 95% confidence.

To determine critical LOD scores, we simulated paternity assignments for 100,000 offspring (the recommended number) using the following parameters: 122 candidate males, 67% of candidate males sampled, and the default of 1% of loci mistyped. We approximated the proportion of candidate males sampled by estimating the number of males of both species that held neighboring territories to the sampled males but were never caught. The proportion of typed loci for the simulation was 0.972. As known mothers (confirmed by catching females at the nest) were sampled for 88% of offspring, we included known mothers in the analysis and evaluated CERVUS assignments using trio LOD scores, which take into account potential genotyping errors and the genotypes of known mothers when assigning paternity. Our total sample included 82 candidate males. We accepted assignments if the number of mismatches between the assigned male and his offspring was less than or equal to the maximum observed number of mismatches between a mother and her known offspring [as in (*59*); max = 8, <3% of 281 loci; table S4]. We assigned 51 of 77 nestlings (66%) to a candidate father with 95% confidence.

Feather coloration

We collected feathers from four plumage patches across the body (crown, throat, belly, and rump) from 68 individuals of *S. hypoxantha* (46 males and 22 females) and 61 individuals of *S. iberaensis* (41 males and 20 females) to examine plumage coloration. We stacked 10 to

Downloaded from http://science.sciencemag.org/ on March 25, 2021

15 feathers from each plumage patch on a nonreflective background surface (Flock Paper, Edmund Optics) to mimic their placement on the body of the bird. Reflectance data were generated relative to a white standard (WS-1-SL, Ocean Optics) and a dark standard (all light omitted) with an Ocean Optics Flame spectrometer connected to an Ocean Optics PX-2 pulsed xenon light source. We used the OceanView software package (version 1.6.7, Ocean Optics) to record the reflectance data, averaging 20 scans per measurement. For each plumage patch, we took three measurements per individual and averaged the measurements prior to subsequent analysis. We used the R package *pavo* to compare the reflectance curves and degree of overlap in tetrahedral color space for each plumage patch between individuals of *S. hypoxantha* and *S. iberaensis* (*67*).

Behavioral experiment

From October to December 2019, we located males of *S. hypoxantha* (N = 40) and *S. iberaensis* (N = 36) that were actively singing on their territories in the San Nicolás Reserve and carried out a behavioral experiment in which we presented them with the following five treatments: (i) conspecific mount and song, (ii) heterospecific capuchino mount and conspecific song, (iii) conspecific mount and heterospecific capuchino song, (iv) heterospecific capuchino mount and heterospecific capuchino song, and (v) heterospecific control mount and song. Although *S. hypoxantha* and *S. iberaensis* form social pairs during October–November, our paternity data indicate that extra-pair mating continues throughout December in the San Nicolás Reserve. Male responses to mount presentation and song playback are often used to infer the importance of pre-mating isolation between divergent taxa (*68*–*72*), as numerous studies have found that the traits used by males to recognize sexual competitors are also used in female mate choice (*73*–*75*). For the heterospecific control, we followed the methods of (*14*) and used *S. collaris*, which is closely related to our focal species but is not a capuchino seedeater (*14*, *76*). *S. collaris* breeds in sympatry and occupies a very similar ecological niche to *S. hypoxantha* and *S. iberaensis* (*77*, *78*). The heterospecific control treatment thus attempts to discriminate between aggressive responses to ecological and sexual competitors, given that all three species are grassland birds that feed on the seeds of tall grasses, such as *Paspalum durifolium* (Poaceae) and *Andropogon lateralis* (Poaceae), which dominate the landscape in the San Nicolás Reserve (*24*, *79*). In particular, an elevated response to conspecific traits relative to the stimuli of the heterospecific capuchino and control would indicate that (i) capuchinos recognize members of their own species as sexual competitors, and (ii) the conspecific traits that elicit an elevated response are involved in male-male competition and potentially female choice (*73*–*75*). In contrast, a similarly aggressive response to conspecific and heterospecific capuchino stimuli would suggest that capuchinos do not discriminate between *S. hypoxantha* and *S. iberaensis*, recognizing males of both species as sexual and/or ecological competitors. Finally, an aggressive response to the control *S. collaris* stimuli would suggest that this more distantly related species, which is not a sexual competitor, elicits a response because it is recognized as an ecological competitor.

We recorded the geographic coordinates of each trial and tested focal males with as many treatments as possible (up to five treatments) by returning to the same geographic location multiple times. Trials performed with the same focal males were separated by at least 1 day, and the order in which treatments were presented was randomized. In addition, we randomized the order in which stimuli were presented across trials and ensured that the mounts (two of *S. hypoxantha*, two of *S. iberaensis*, and two of *S. collaris*) and playback files (10 of *S. hypoxantha*, 10 of *S. iberaensis*, and five of *S. collaris*) were presented an equal number of times. Sixteen of the 76 focal males (21%) were color-banded from our field work in previous years. In addition, capuchino seedeaters exhibit a considerable degree of intraspecific variation in plumage coloration, which is likely associated with age, and only sing within their territories. Thus, by returning to the same location where a male was previously observed singing, and using color bands or plumage to identify individuals, we could be confident that the same individual was tested in subsequent trials.

During each trial, we located the focal male and set up the mount ~1 to 2 m off the ground <35 m from the focal male on a thin pole near vegetation suitable for perching. We hid a compact speaker (JBL Flip 5) in the vegetation under the mount and connected the speaker to a phone through Bluetooth to start the playback recordings. Each trial lasted a total of 5 min (the duration of the playback file), with the same observer (always S.P.T., for consistency in scoring behavioral responses) standing 20 m away from the mount. We generated video recordings of each trial with a DSLR camera (Canon EOS 7D) and dictated vocalizations and behaviors into the camera during the trials. We recorded the following behavioral responses: the number of flights and amount of time spent at various distances from the mount, the number of attacks and amount of time spent attacking the mount, and the amount of time spent singing by each focal male, using the 2-m pole on which the mount was placed to estimate distance from the mount. Although females do not assist with territorial defense in capuchino seedeaters, we noted whether or not a female was observed during each trial in case female presence influences male response to territorial intrusion. Females were observed in 53 trials (22%). In total, we presented 32 males (16 *S. hypoxantha* and 16 *S. iberaensis*) with all five treatments and 44 males (24 *S. hypoxantha* and 20 *S. iberaensis*) with fewer than five treatments, for a total of 240 trials (24 trials per treatment for each species).

We ran a PCA on the correlation matrix of the behavioral response variables using the R package *vegan* to reduce the dimensionality of the behavioral data. The PCA identified three axes of variation (eigenvalues > 1) that collectively explained 79% of the variation in behavioral responses (PC1, 43%; PC2, 20%; PC3, 16%). All input variables associated with male aggression (e.g., number of flights near the mount, proportion of time spent near the mount, and number of attacks at the mount) loaded positively on PC1, whereas proportion of time spent singing and proportion of time spent >6 m from the mount loaded negatively on PC1 (fig. S15C), indicating that PC1 represented a reasonable overall summary of aggression. We therefore extracted PC1 to generate a response intensity score for each trial. In addition, we classified all trials as displaying attack behavior ("1") or not ("0"), with attack behavior defined as either swooping at or making direct contact with the mount, to examine a direct indicator of aggression. We carried out parallel analyses with response intensity (i.e., PC1) and attack behavior as dependent variables using R version 3.5.2 (*43*) and fit generalized linear mixed models (GLMMs) with the R packages *lme4* (for linear mixed models) and *glmmTMB* (for mixed logistic regression models) to analyze the responses of territory owners to mount presentation and song playback (*80*, *81*).

Because territorial males typically did not respond to the heterospecific control (*S. collaris*) stimuli, we ran separate analyses with and without the control trials [as in (*82*)]. Excluding the control trials, we first ran GLMMs examining the effects of species, plumage, and song (fixed effects) on (i) response intensity (PC1) and (ii) attack behavior (whether or not the mount was attacked at any point during the trial). We used a mixed logistic regression model with a binomial distribution and logit link function to model attack behavior, which had a binary outcome (0 or 1). Preliminary models included treatment order, male ID, female presence (0 or 1), mount ID, and playback ID as random effects, with mount ID and playback ID nested within each plumage and song type, respectively, in order to control for repeated measures from individuals and mount/playback exemplar effects. We calculated a 95% confidence interval (CI) around

Downloaded from http://science.sciencemag.org/ on March 25, 2021

the estimated standard deviation explained by the random effects using the *confint()* function from the R stats package. We excluded random effects from the model if the lower end of the CI reached zero, indicating that the effect did not account for variation in the model (e.g., treatment order, mount ID, and playback ID), retaining male ID in the model of attack behavior and male ID and female presence in the model of response intensity.

In addition, we included the heterospecific control trials to run a GLMM for each focal species that tested the effect of treatment group on response intensity (PC1), incorporating male ID and female presence as random effects. We used the R package *emmeans* to run post hoc pairwise comparisons between treatment groups using Tukey's honestly significant difference (HSD) test (*83*). Again, treatment order, mount ID, playback ID, and female presence (in the case of *S. hypoxantha*) had 95% CIs that reached zero when included as random effects in the preliminary models and were therefore excluded from the final analyses. We verified the assumptions of the linear mixed models by generating Q-Q plots and plotting the residuals versus the fitted values.

Abundance estimates

To estimate whether *S. iberaensis* has increased in abundance across its breeding range since the species' first records in 2001 (*18*), we downloaded eBird data through January 2020 from the February 2020 release of the eBird Basic Dataset (*84*). The downloaded dataset contained all available data for the control used in the behavioral experiment (*S. collaris*) and the seven capuchino species (*S. iberaensis*, *S. hypoxantha*, *S. cinnamomea*, *S. palustris*, *S. pileata*, *S. ruficollis*, and *S. hypochroma*) that breed in Iberá National Park (*17*), as well as the sampling event data (needed to infer nondetection records). eBird is an online database where scientists, researchers, and amateur naturalists can upload avian observations (*85*). We filtered the data for each species using the R package *auk* (*86*) to exclude records from incomplete checklists (i.e., checklists in which some identified species were not reported) and observations that fell outside of a bounding box around the area encompassing all observations of *S. iberaensis* in Argentina and Paraguay (the central range of *S. iberaensis*), retaining only a single checklist from each set of non-independent ("shared") checklists. We then inferred nondetection records (i.e., "zero-filled the data") using the *auk* package to create presence/absence data for each species. To more precisely define the spatial area of interest, we converted the presence-only data from *S. iberaensis* into a spatial object and generated a convex hull polygon around the distribution of *S. iberaensis* records using the function *gbuffer()* in the R package *rgeos* (*87*), adding a buffer of 1 map unit (with data in a South America Albers equal-area conic projection) outside of these locations; we only retained records of observations that fell within this polygon of interest. We then placed temporal restrictions on the remaining data, only retaining records from October to February, when capuchino seedeaters are present on the breeding grounds, and records beginning with the austral summer that spanned the years 2013–2014, the first summer for which multiple observations of *S. iberaensis* existed in the eBird database.

After processing the data, we examined whether there have been any systematic changes in the reporting rates of the seven capuchino seedeater species over the past decade in order to assess whether *S. iberaensis* has increased in prevalence relative to other capuchino species. We modeled changes in prevalence by fitting generalized additive models (GAMs) [using the R package *mgcv* (*88*)], in which the probability of reporting of the focal species was modeled as a function of the calendar year at the end of each austral summer. GAMs are able to identify arbitrary, continuous patterns of change through time, rather than forcing specific patterns onto the data. We used additional smoothing terms to account for variation in observation effort as described by the following variables: observation date, distance traveled, and duration of the observation period. We compared the GAM results for each capuchino species to determine whether (i) there was a significant change in the reporting probability of each species over time, and (ii) whether reporting probability consistently increased from 2014 to 2019.

REFERENCES AND NOTES

1. R. Butlin *et al*., What do we need to know about speciation? *Trends Ecol. Evol.* **27**, 27–39 (2012). doi: 10.1016/j.tree.2011.09.002; pmid: 21978464
2. J. M. Sobel, M. A. Streisfeld, Strong premating reproductive isolation drives incipient speciation in *Mimulus aurantiacus*. *Evolution* **69**, 447–461 (2015). doi: 10.1111/evo.12589; pmid: 25545789
3. A. C. R. Lackey, J. W. Boughman, Evolution of reproductive isolation in stickleback fish. *Evolution* **71**, 357–372 (2017). doi: 10.1111/evo.13114; pmid: 27901265
4. J. A. C. Uy, D. E. Irwin, M. S. Webster, Behavioral Isolation and Incipient Speciation in Birds. *Annu. Rev. Ecol. Evol. Syst.* **49**, 1–24 (2018). doi: 10.1146/annurev-ecolsys-110617-062646
5. T. D. Price, M. M. Bouvier, The evolution of F1 postzygotic incompatibilities in birds. *Evolution* **56**, 2083–2089 (2002). doi: 10.1111/j.0014-3820.2002.tb00133.x; pmid: 12449494
6. J. A. Coyne, H. A. Orr, Patterns of speciation in *Drosophila*. *Evolution* **43**, 362–381 (1989). doi: 10.1111/j.1558-5646.1989.tb04233.x; pmid: 28568554
7. M. Xu, K. L. Shaw, Genetic coupling of signal and preference facilitates sexual isolation during rapid speciation. *Proc. R. Soc. B* **286**, 20191607 (2019). doi: 10.1098/rspb.2019.1607; pmid: 31640515
8. O. Seehausen *et al*., Speciation through sensory drive in cichlid fish. *Nature* **455**, 620–626 (2008). doi: 10.1038/nature07285; pmid: 18833272
9. P. R. Grant, B. R. Grant, Role of sexual imprinting in assortative mating and premating isolation in Darwin's finches. *Proc. Natl. Acad. Sci. U.S.A.* **115**, E10879–E10887 (2018). doi: 10.1073/pnas.1813662115; pmid: 30348758
10. T. C. Mendelson, Sexual isolation evolves faster than hybrid inviability in a diverse and sexually dimorphic genus of fish (Percidae: Etheostoma). *Evolution* **57**, 317–327 (2003). doi: 10.1111/j.0014-3820.2003.tb00266.x; pmid: 12683528
11. L. Campagna *et al*., Repeated divergent selection on pigmentation genes in a rapid finch radiation. *Sci. Adv.* **3**, e1602404 (2017). doi: 10.1126/sciadv.1602404; pmid: 28560331
12. L. Campagna *et al*., Rapid phenotypic evolution during incipient speciation in a continental avian radiation. *Proc. R. Soc. B* **279**, 1847–1856 (2012). doi: 10.1098/rspb.2011.2170; pmid: 22130601
13. O. M. Selz, M. E. R. Pierotti, M. E. Maan, C. Schmid, O. Seehausen, Female preference for male color is necessary and sufficient for assortative mating in 2 cichlid sister species. *Behav. Ecol.* **25**, 612–626 (2014). doi: 10.1093/beheco/aru024
14. P. Benites, L. Campagna, P. L. Tubaro, Song-based species discrimination in a rapid Neotropical radiation of grassland seedeaters. *J. Avian Biol.* **46**, 55–62 (2015). doi: 10.1111/jav.00447
15. C. A. B. Medolago, M. C. Costa, L. F. Silveira, M. R. Francisco, Hybridization between two recently diverged Neotropical passerines: The Pearly-bellied Seedeater *Sporophila pileata*, and the Copper Seedeater *S. bouvreuil* (Aves, Passeriformes, Thraupidae). *PLOS ONE* **15**, e0229714 (2020). doi: 10.1371/journal.pone.0229714; pmid: 32218563
16. L. Campagna, P. Rodriguez, J. C. Mazzulla, Transgressive phenotypes and evidence of weak postzygotic isolation in F1 hybrids between closely related capuchino seedeaters. *PLOS ONE* **13**, e0199113 (2018). doi: 10.1371/journal.pone.0199113; pmid: 29902247
17. Birdlife International, *IUCN Red List for Birds* (2020); www.birdlife.org.
18. A. S. Di Giacomo, C. Kopuchian, Una nueva especie de capuchino (*Sporophila*: Thraupidae) de los Esteros del Iberá, Corrientes, Argentina. *Nuestras Aves* **61**, 3–5 (2016).
19. M. Repenning, C. S. Fontana, A New Species of Gray Seedeater (Emberizidae: *Sporophila*) from Upland Grasslands of Southern Brazil. *Auk* **130**, 791–803 (2013). doi: 10.1525/auk.2013.12167
20. M. Abolins-Abols *et al*., Differential gene regulation underlies variation in melanic plumage coloration in the dark-eyed junco (*Junco hyemalis*). *Mol. Ecol.* **27**, 4501–4515 (2018). doi: 10.1111/mec.14878; pmid: 30252177
21. I. C. Cuthill *et al*., Ultraviolet Vision in Birds. *Adv. Stud. Behav.* **29**, 159–214 (2000). doi: 10.1016/S0065-3454(08)60105-9
22. P. Benites, M. D. Eaton, D. A. Lijtmaer, S. C. Lougheed, P. L. Tubaro, Analysis from avian visual perspective reveals plumage colour differences among females of capuchino seedeaters (*Sporophila*). *J. Avian Biol.* **41**, 597–602 (2010). doi: 10.1111/j.1600-048X.2010.05205.x
23. S. C. Griffith, I. P. F. Owens, K. A. Thuman, Extra pair paternity in birds: A review of interspecific variation and adaptive function. *Mol. Ecol.* **11**, 2195–2212 (2002). doi: 10.1046/j.1365-294X.2002.01613.x; pmid: 12406233
24. S. P. Turbek, M. Browne, C. Pasian, A. S. Di Giacomo, First nest description of the Iberá Seedeater (*Sporophila iberaensis*). *Wilson J. Ornithol.* **131**, 156–160 (2019). doi: 10.1676/17-35
25. D. Wheatcroft, A. Qvarnström, Genetic divergence of early song discrimination between two young songbird species. *Nat. Ecol. Evol.* **1**, 192 (2017). doi: 10.1038/s41559-017-0192
26. D. A. Marques, J. I. Meier, O. Seehausen, A Combinatorial View on Speciation and Adaptive Radiation. *Trends Ecol. Evol.* **34**, 531–544 (2019). doi: 10.1016/j.tree.2019.02.008; pmid: 30885412
27. J. I. Meier, D. A. Marques, C. E. Wagner, L. Excoffier, O. Seehausen, Genomics of Parallel Ecological Speciation in Lake Victoria Cichlids. *Mol. Biol. Evol.* **35**, 1489–1506 (2018). doi: 10.1093/molbev/msy051; pmid: 29617828
28. D. J. Howard, Reinforcement: Origin, dynamics, and fate of an evolutionary process. In *Hybrid Zones and the Evolutionary Process*, R. G. Harrison, Ed. (Oxford Univ. Press, 1993), pp. 46–69.
29. H. Ellegren, Genomic evidence for a large-Z effect. *Proc. R. Soc. B* **276**, 361–366 (2009). doi: 10.1098/rspb.2008.1135; pmid: 18826931
30. S. Lamichhaney *et al*., Rapid hybrid speciation in Darwin's finches. *Science* **359**, 224–228 (2018). doi: 10.1126/science.aao4593; pmid: 29170277
31. E. B. Rosenblum *et al*., Goldilocks Meets Santa Rosalia: An Ephemeral Speciation Model Explains Patterns of Diversification Across Time Scales. *Evol. Biol.* **39**, 255–261 (2012). doi: 10.1007/s11692-012-9171-x; pmid: 22707806
32. J. M. C. da Silva, Seasonal movements and conservation of seedeaters of the genus *Sporophila* in South America. *Stud. Avian Biol.* **19**, 272–280 (1999).
33. S. Andrews, fastqc, a Quality Control Tool for High Throughput Sequence Data (2010); www.bioinformatics.babraham.ac.uk/projects/fastqc.

Downloaded from http://science.sciencemag.org/ on March 25, 2021

34. M. Schubert, S. Lindgreen, L. Orlando, AdapterRemoval v2: Rapid adapter trimming, identification, and read merging. *BMC Res. Notes* **9**, 88 (2016). doi: 10.1186/s13104-016-1900-2; pmid: 26868221
35. B. Langmead, S. L. Salzberg, Fast gapped-read alignment with Bowtie 2. *Nat. Methods* **9**, 357–359 (2012). doi: 10.1038/nmeth.1923; pmid: 22388286
36. F. García-Alcalde *et al*., Qualimap: Evaluating next-generation sequencing alignment data. *Bioinformatics* **28**, 2678–2679 (2012). doi: 10.1093/bioinformatics/bts503; pmid: 22914218
37. H. Li *et al*., The Sequence Alignment/Map format and SAMtools. *Bioinformatics* **25**, 2078–2079 (2009). doi: 10.1093/bioinformatics/btp352; pmid: 19505943
38. Broad Institute, Picard Toolkit (2018); http://broadinstitute.github.io/picard.
39. A. McKenna *et al*., The Genome Analysis Toolkit: A MapReduce framework for analyzing next-generation DNA sequencing data. *Genome Res.* **20**, 1297–1303 (2010). doi: 10.1101/gr.107524.110; pmid: 20644199
40. P. Danecek *et al*., The variant call format and VCFtools. *Bioinformatics* **27**, 2156–2158 (2011). doi: 10.1093/bioinformatics/btr330; pmid: 21653522
41. S. Turner, qqman: An R package for visualizing GWAS results using Q-Q and Manhattan plots. *J. Open Source Softw.* **3**, 731 (2018). doi: 10.21105/joss.00731
42. X. Zheng *et al*., A high-performance computing toolset for relatedness and principal component analysis of SNP data. *Bioinformatics* **28**, 3326–3328 (2012). doi: 10.1093/bioinformatics/bts606; pmid: 23060615
43. R: A Language and Environment for Statistical Computing (2018); www.r-project.org.
44. S. Purcell *et al*., PLINK: A tool set for whole-genome association and population-based linkage analyses. *Am. J. Hum. Genet.* **81**, 559–575 (2007). doi: 10.1086/519795; pmid: 17701901
45. M. G. Grabherr *et al*., Genome-wide synteny through highly sensitive sequence alignment: Satsuma. *Bioinformatics* **26**, 1145–1151 (2010). doi: 10.1093/bioinformatics/btq102; pmid: 20208069
46. M. Meyer, T. Munzner, H. Pfister, MizBee: A multiscale synteny browser. *IEEE Trans. Vis. Comput. Graph.* **15**, 897–904 (2009). doi: 10.1109/TVCG.2009.167; pmid: 19834152
47. S. F. Altschul, W. Gish, W. Miller, E. W. Myers, D. J. Lipman, Basic local alignment search tool. *J. Mol. Biol.* **215**, 403–410 (1990). doi: 10.1016/S0022-2836(05)80360-2; pmid: 2231712
48. A. Siepel *et al*., Evolutionarily conserved elements in vertebrate, insect, worm, and yeast genomes. *Genome Res.* **15**, 1034–1050 (2005). doi: 10.1101/gr.3715005; pmid: 16024819
49. W. J. Kent *et al*., The human genome browser at UCSC. *Genome Res.* **12**, 996–1006 (2002). doi: 10.1101/gr.229102; pmid: 12045153
50. W. J. Kent, BLAT—The BLAST-like alignment tool. *Genome Res.* **12**, 656–664 (2002). doi: 10.1101/gr.229202; pmid: 11932250
51. C. Hahn, L. Bachmann, B. Chevreux, Reconstructing mitochondrial genomes directly from genomic next-generation sequencing reads—A baiting and iterative mapping approach. *Nucleic Acids Res.* **41**, e129 (2013). doi: 10.1093/nar/gkt371; pmid: 23661685
52. M. Kearse *et al*., Geneious Basic: An integrated and extendable desktop software platform for the organization and analysis of sequence data. *Bioinformatics* **28**, 1647–1649 (2012). doi: 10.1093/bioinformatics/bts199; pmid: 22543367
53. J. W. Leigh, D. Bryant, POPART: Full-feature software for haplotype network construction. *Methods Ecol. Evol.* **6**, 1110–1116 (2015). doi: 10.1111/2041-210X.12410
54. P. D. N. Hebert, S. Ratnasingham, J. R. de Waard, Barcoding animal life: cytochrome c oxidase subunit 1 divergences among closely related species. *Proc. R. Soc. B* **270**, S96–S99 (2003). doi: 10.1111/2041-210X.12410
55. K. C. R. Kerr, D. A. Lijtmaer, A. S. Barreira, P. D. N. Hebert, P. L. Tubaro, Probing evolutionary patterns in neotropical birds through DNA barcodes. *PLOS ONE* **4**, e4379 (2009). doi: 10.1371/journal.pone.0004379; pmid: 19194495
56. L. Campagna *et al*., DNA barcodes provide new evidence of a recent radiation in the genus *Sporophila* (Aves: Passeriformes). *Mol. Ecol. Resour.* **10**, 449–458 (2010). doi: 10.1111/j.1755-0998.2009.02799.x; pmid: 21565044
57. A. Stamatakis, RAxML version 8: A tool for phylogenetic analysis and post-analysis of large phylogenies. *Bioinformatics* **30**, 1312–1313 (2014). doi: 10.1093/bioinformatics/btu033; pmid: 24451623
58. A. M. Kozlov, D. Darriba, T. Flouri, B. Morel, A. Stamatakis, RAxML-NG: A fast, scalable and user-friendly tool for maximum likelihood phylogenetic inference. *Bioinformatics* **35**, 4453–4455 (2019). doi: 10.1093/bioinformatics/btz305; pmid: 31070718
59. D. J. Thrasher, B. G. Butcher, L. Campagna, M. S. Webster, I. J. Lovette, Double-digest RAD sequencing outperforms microsatellite loci at assigning paternity and estimating relatedness: A proof of concept in a highly promiscuous bird. *Mol. Ecol. Resour.* **18**, 953–965 (2018). doi: 10.1111/1755-0998.12771; pmid: 29455472
60. J. Catchen, P. A. Hohenlohe, S. Bassham, A. Amores, W. A. Cresko, Stacks: An analysis tool set for population genomics. *Mol. Ecol.* **22**, 3124–3140 (2013). doi: 10.1111/mec.12354; pmid: 23701397
61. K. Okonechnikov, O. Golosova, M. Fursov, UGENE Team, Unipro UGENE: A unified bioinformatics toolkit. *Bioinformatics* **28**, 1166–1167 (2012). doi: 10.1093/bioinformatics/bts091; pmid: 22368248
62. S. R. Browning, B. L. Browning, Rapid and accurate haplotype phasing and missing-data inference for whole-genome association studies by use of localized haplotype clustering. *Am. J. Hum. Genet.* **81**, 1084–1097 (2007). doi: 10.1086/521987; pmid: 17924348
63. J. Oksanen *et al*., Vegan: community ecology package. R package version 1.17-4 (2010).
64. L. J. Revell, phytools: An R package for phylogenetic comparative biology (and other things). *Methods Ecol. Evol.* **3**, 217–223 (2012). doi: 10.1111/j.2041-210X.2011.00169.x
65. J. Chifman, L. Kubatko, Quartet inference from SNP data under the coalescent model. *Bioinformatics* **30**, 3317–3324 (2014). doi: 10.1093/bioinformatics/btu530; pmid: 25104814
66. S. T. Kalinowski, M. L. Taper, T. C. Marshall, Revising how the computer program CERVUS accommodates genotyping error increases success in paternity assignment. *Mol. Ecol.* **16**, 1099–1106 (2007). doi: 10.1111/j.1365-294X.2007.03089.x; pmid: 17305863
67. R. Maia, C. M. Eliason, P.-P. Bitton, S. M. Doucet, M. D. Shawkey, pavo: An R package for the analysis, visualization and organization of spectral data. *Methods Ecol. Evol.* **4**, 906–913 (2013). doi: 10.1111/2041-210X.12069
68. D. E. Irwin, S. Bensch, T. D. Price, Speciation in a ring. *Nature* **409**, 333–337 (2001). doi: 10.1038/35053059; pmid: 11201740
69. B. R. Grant, P. R. Grant, Lack of premating isolation at the base of a phylogenetic tree. *Am. Nat.* **160**, 1–19 (2002). doi: 10.1086/339987; pmid: 18707495
70. B. R. Grant, P. R. Grant, Simulating secondary contact in allopatric speciation: An empirical test of premating isolation. *Biol. J. Linn. Soc. London* **76**, 545–556 (2002). doi: 10.1046/j.1095-8312.2002.00076.x
71. C. N. Balakrishnan, M. D. Sorenson, Song discrimination suggests premating isolation among sympatric indigobird species and host races. *Behav. Ecol.* **17**, 473–478 (2006). doi: 10.1093/beheco/arj052
72. J. A. C. Uy, R. G. Moyle, C. E. Filardi, Z. A. Cheviron, Difference in plumage color used in species recognition between incipient species is linked to a single amino acid substitution in the melanocortin-1 receptor. *Am. Nat.* **174**, 244–254 (2009). doi: 10.1086/600084; pmid: 19489704
73. M. C. Baker, Response of Male Indigo and Lazuli Buntings and Their Hybrids To Song Playback in Allopatric and Sympatric Populations. *Behaviour* **119**, 225–242 (1991). doi: 10.1163/156853991X00454
74. M. C. Baker, A. E. M. Baker, Reproductive behavior of female buntings: Isolating mechanisms in a hybridizing pair of species. *Evolution* **44**, 332–338 (1990). doi: 10.1111/j.1558-5646.1990.tb05202.x; pmid: 28564380
75. M. A. Patten, J. T. Rotenberry, M. Zuk, Habitat selection, acoustic adaptation, and the evolution of reproductive isolation. *Evolution* **58**, 2144–2155 (2004). doi: 10.1111/j.0014-3820.2004.tb01593.x; pmid: 15562681
76. N. A. Mason, K. J. Burns, Molecular phylogenetics of the Neotropical seedeaters and seed-finches (*Sporophila*, *Oryzoborus*, *Dolospingus*). *Ornitol. Neotrop.* **24**, 139–155 (2013).
77. A. S. Di Giacomo, *Áreas Importantes para la Conservación de las Aves en la Argentina: Sitios Prioritarios para la Conservación de la Biodiversidad* (Aves Argentinas/Asociación Ornitológica del Plata, Buenos Aires, 2005).
78. A. G. Di Giacomo, S. F. Krapovickas, *Historia natural y paisaje de la Reserva El Bagual, Formosa, Argentina* (Aves Argentinas/Asociación Ornitológica del Plata, Buenos Aires, 2005).
79. J. del Hoyo, A. Elliott, J. Sargatal, D. A. Christie, G. Kirwan, *Handbook of the Birds of the World Alive* (Lynx, Barcelona, 2020); www.hbw.com/.
80. D. Bates, M. Mächler, B. Bolker, S. Walker, Fitting Linear Mixed-Effects Models Using lme4. *J. Stat. Softw.* **67**, 1–48 (2015). doi: 10.18637/jss.v067.i01
81. M. E. Brooks *et al*., glmmTMB balances speed and flexibility among packages for zero-inflated generalized linear mixed modeling. *R J.* **9**, 378–400 (2017). doi: 10.32614/RJ-2017-066
82. J. A. C. Uy, R. G. Moyle, C. E. Filardi, Plumage and song differences mediate species recognition between incipient flycatcher species of the Solomon Islands. *Evolution.* **63**, 153–164 (2009). doi: 10.1111/j.1558-5646.2008.00530.x; pmid: 18803681
83. R. Lenth, H. Singmann, J. Love, Emmeans: Estimated marginal means, aka least-squares means. R package version 1.1 (2018).
84. eBird Basic Dataset. Version: EBD_relJan-2020 (Cornell Lab of Ornithology, 2020).
85. B. L. Sullivan *et al*., The eBird enterprise: An integrated approach to development and application of citizen science. *Biol. Conserv.* **169**, 31–40 (2014). doi: 10.1016/j.biocon.2013.11.003
86. M. Strimas-Mackey, E. Miller, W. Hochachka, auk: eBird Data Extraction and Processing with AWK. R package version 0.3 (2017).
87. R. Bivand, C. Rundel, rgeos: interface to geometry engine-open source (GEOS). R package version 0.3-23 (2017).
88. S. N. Wood, Fast stable restricted maximum likelihood and marginal likelihood estimation of semiparametric generalized linear models. *J. R. Stat. Soc. B* **73**, 3–36 (2011). doi: 10.1111/j.1467-9868.2010.00749.x
89. E. T. Domyan *et al*., Epistatic and combinatorial effects of pigmentary gene mutations in the domestic pigeon. *Curr. Biol.* **24**, 459–464 (2014). doi: 10.1016/j.cub.2014.01.020; pmid: 24508169
90. E. E. Kenny *et al*., Melanesian blond hair is caused by an amino acid change in TYRP1. *Science* **336**, 554–554 (2012). doi: 10.1126/science.1217849; pmid: 22556244
91. J. Li *et al*., A missense mutation in TYRP1 causes the chocolate plumage color in chicken and alters melanosome structure. *Pigment Cell Melanoma Res.* **32**, 381–390 (2019). doi: 10.1111/pcmr.12753; pmid: 30457703
92. L. A. Lyons, I. T. Foe, H. C. Rah, R. A. Grahn, Chocolate coated cats: TYRP1 mutations for brown color in domestic cats. *Mamm. Genome* **16**, 356–366 (2005). doi: 10.1007/s00335-004-2455-4; pmid: 16104383
93. R. A. Sturm, T. N. Frudakis, Eye colour: Portals into pigmentation genes and ancestry. *Trends Genet.* **20**, 327–332 (2004). doi: 10.1016/j.tig.2004.06.010; pmid: 15262401
94. M. Visser, M. Kayser, F. Grosveld, R.-J. Palstra, Genetic variation in regulatory DNA elements: The case of OCA2 transcriptional regulation. *Pigment Cell Melanoma Res.* **27**, 169–177 (2014). doi: 10.1111/pcmr.12210; pmid: 24387780
95. H. Klaassen, Y. Wang, K. Adamski, N. Rohner, J. E. Kowalko, CRISPR mutagenesis confirms the role of oca2 in melanin pigmentation in *Astyanax mexicanus*. *Dev. Biol.* **441**, 313–318 (2018). doi: 10.1016/j.ydbio.2018.03.014; pmid: 29555241
96. M. Visser, M. Kayser, R.-J. Palstra, HERC2 rs12913832 modulates human pigmentation by attenuating chromatin-loop formation between a long-range enhancer and the OCA2 promoter. *Genome Res.* **22**, 446–455 (2012). doi: 10.1101/gr.128652.111; pmid: 22234890

ACKNOWLEDGMENTS

We thank C. Pasian, B. Rodríguez-Quintana, and B. Rodrigues do Amaral for field assistance; E. Turbek for generating the mounts; and feedback from the Taylor, Safran, and Lovette lab groups. **Funding:** Supported by grants from AGA, NGS, APS, ASN, WOS, BOU, AOS, SSB, CU-Boulder, NSF GRFP (S.P.T.), NSF (DEB-1555769) (I.J.L.), FAPESP-2017/23548-2 and CNPq-308337/2019-0 (L.F.S.), ANPCyT and CONICET (A.S.D.G. and D.A.L.), and NGC (M.B.). **Author contributions:** Designed project: S.P.T., R.J.S., L.C. Performed fieldwork: S.P.T., M.B., A.S.D.G., C.K. Obtained genomic data: S.P.T., L.C., I.J.L., C.E., D.A.L., P.L.T., L.F.S. Analyzed genomic data: S.P.T., L.C. Performed and analyzed behavioral experiments: S.P.T. Analyzed eBird data: W.M.H. Supervised research: R.J.S., S.A.T., L.C. Wrote manuscript: S.P.T., L.C. with edits from all authors. **Competing interests:** None. **Data and materials availability:** Dryad (doi:10.5061/dryad.cjsxksn4h), NCBI (BioProject-PRJNA382416).

SUPPLEMENTARY MATERIALS

science.sciencemag.org/content/371/6536/eabc0256/suppl/DC1
Materials and Methods
Supplementary Text
Figs. S1 to S20
Tables S1 to S5
References (*97*–*108*)

3 April 2020; accepted 21 January 2021
10.1126/science.abc0256

Downloaded from http://science.sciencemag.org/ on March 25, 2021

Science

Rapid speciation via the evolution of pre-mating isolation in the Iberá Seedeater

Sheela P. Turbek, Melanie Browne, Adrián S. Di Giacomo, Cecilia Kopuchian, Wesley M. Hochachka, Cecilia Estalles, Darío A. Lijtmaer, Pablo L. Tubaro, Luís Fábio Silveira, Irby J. Lovette, Rebecca J. Safran, Scott A. Taylor and Leonardo Campagna

Science **371** (6536), eabc0256.
DOI: 10.1126/science.abc0256

Choosy females drive isolation

Rapid radiations of recently diverged species represent an excellent opportunity for exploring drivers of speciation. The capuchino seedeaters, a group of South American birds, include a number of species that, in the field, are often discernable only through male plumage and song. Turbek *et al.* used genomes and behavioral experiments to identify potential isolating factors in two members of this group and found that, though entirely sympatric, females mated only with conspecific males and that only a few genes differed between the species (see the Perspective by Jarvis). Thus, a small reshuffling of genes and reinforcement through mate choice has driven divergence in these overlapping and very similar species.

Science, this issue p. eabc0256; see also p. 1312

ARTICLE TOOLS http://science.sciencemag.org/content/371/6536/eabc0256

SUPPLEMENTARY MATERIALS http://science.sciencemag.org/content/suppl/2021/03/24/371.6536.eabc0256.DC1

RELATED CONTENT http://science.sciencemag.org/content/sci/371/6536/1312.full

REFERENCES This article cites 93 articles, 11 of which you can access for free
http://science.sciencemag.org/content/371/6536/eabc0256#BIBL

PERMISSIONS http://www.sciencemag.org/help/reprints-and-permissions

Use of this article is subject to the Terms of Service

Science (print ISSN 0036-8075; online ISSN 1095-9203) is published by the American Association for the Advancement of Science, 1200 New York Avenue NW, Washington, DC 20005. The title *Science* is a registered trademark of AAAS.

Copyright © 2021 The Authors, some rights reserved; exclusive licensee American Association for the Advancement of Science. No claim to original U.S. Government Works

Downloaded from http://science.sciencemag.org/ on March 25, 2021